Quasiparticle band structure of silicon carbide polytypes

Bernd Wenzien, Peter Käckell, and Friedhelm Bechstedt
Friedrich-Schiller-Universität, Institut für Festkörpertheorie und Theoretische Optik, Max-Wien-Platz 1, 07743 Jena, Germany

Giancarlo Cappellini
Universita di Cagliari, Istituto di Fisica, Facolte di Medicine e Chirugie, Via della Pineta 77, 09125 Cagliari, Italy
(Received 1 February 1995; revised manuscript received 5 July 1995)

The *ab initio* pseudopotential method within the local-density approximation and the quasiparticle approach have been used to investigate the electronic excitation properties of hexagonal ($6H$, $4H$, $2H$) and zinc-blende ($3C$) silicon carbide. The quasiparticle shifts added to the density-functional eigenvalues are calculated using a model dielectric function and an approximate treatment of the electron self-energy concerning local-field effects and dynamical screening. The inverse dielectric function and the auxiliary function are generalized to hexagonal crystals. Good agreement with the experimental results is obtained for the minimum indirect energy gaps. The **k** space location of the corresponding conduction-band minima is clarified. Other excitation energies are predicted. The influence of the quasiparticle effects on band discontinuities and the electron effective masses is studied.

I. INTRODUCTION

The various polytypes of silicon carbide (SiC) have attracted extensive experimental and theoretical interest because of their extreme thermal, mechanical, chemical, and electronic properties. Besides the physical question of the reasons for the polytypism, the principal driving force for the current resurgence in interest in silicon carbide is its potential as a material for high-power, high-temperature, and high-frequency microelectronic devices resistant to radiation damage.

Experimental studies of the electronic properties of the SiC polytypes have been scarce due to the difficulties concerning the availability of high-quality single crystals or perfect epitaxial layers. Choyke, Hamilton, and Patrick[1,2] found already in 1964 the famous linear relationship between the electronic energy gap and the percentage hexagonality up to 50%, i.e., the increase from zinc-blende $3C$-SiC to the hexagonal polytypes $6H$-SiC and $4H$-SiC, whereas the variation from $4H$- to $2H$-SiC (wurtzite) remains small. For a quantitative explanation of these findings it is necessary to include quasiparticle effects.[3] On the other hand, the basic behavior of the gaps in the polytypes may be already understood without these effects.[4] In a wide energy range optical absorption, reflectivity, spectroscopic ellipsometry, and electroreflectance measurements have been performed for $3C$,[5–7] and $6H$.[8–10] Recently, reflectivity data have been published[11] for the polytypes $3C$, $2H$, $4H$, and $6H$ of interest here. High-resolution band-mapping results exist only for the ΓX direction of $3C$-SiC.[12] Direct measurements of the electron effective masses by means of the cyclotron resonance exist for $3C$ crystals[13] and chemical-vapor-deposited (CVD) layers of $6H$ or $4H$ crystal structure.[14,15]

Recently, the first-principles density-functional theory (DFT) in the local-density approximation (LDA) has been applied not only for studying the ground-state properties of SiC polytypes[16–20] but also for describing their electronic properties.[3,11,17,18,20,21] Meanwhile, there is a unified theoretical picture of the important features of the band structures. The conduction-band minimum state located at the X point for cubic $3C$-SiC changes to the LM line for $6H$ or the M point for $4H$, and then to the K point for the $2H$ structure. However, in the $6H$ case its exact position on the LM line is under discussion.[3,18,20,21] The energy gaps between the valence-band maximum (VBM) at Γ and these states are underestimated but may be brought into rough agreement with experiment after adding a rigid quasiparticle (QP) shift of about 1.1 eV.[3,21,22] For zinc-blende SiC the electronic-structure calculations are already refined and exchange and correlation (XC) of the electron-electron interaction are taken into account on a more sophisticated level.[23,24] For noncubic polytypes such QP calculations are still missing. Further open questions concern details of their conduction-band structure, the effective masses, and the **k** space location of the minimum in the $4H$ case.[25]

In this paper, we present the results of *ab initio* pseudopotential calculations for the electronic structure of $3C$-, $6H$-, $4H$-, and $2H$-SiC which are improved by a proper inclusion of the QP effects. QP band structures are calculated. We discuss the influence of the many-body effects in the excitation spectra on **k** space location, energetical distance, and the curvature of the important band extrema.

II. METHOD

The starting point of the QP band structure calculations is the DFT-LDA, where the electron-ion interaction

is treated by norm-conserving, *ab initio* pseudopotentials of the Bachelet-Hamann-Schlüter type[26] in the fully separable Kleinman-Bylander form.[27] The electron wave functions are expanded in terms of plane waves up to an energy cutoff of 34 Ry. The restriction to the low cutoff arises from the use of softened carbon pseudopotentials. Details of their generating procedure and the discussion of the validity can be found in Refs. 3 and 28. Performing the self-consistent DFT-LDA calculations we apply the computer code FHI93CP of Stumpf and Scheffler.[29] The total energy is minimized by a Car-Parrinello-like procedure[30] with respect to both the ionic and electronic degrees of freedom. As a result we obtain the equilibrium atomic geometry,[19] i.e., in the hexagonal cases the two lattice constants as well as the unit-cell internal positions of the atoms of the atomic basis. Simultaneously the band structures are derived in DFT-LDA quality from the Kohn-Sham eigenvalues.[3]

As typical for semiconductors and insulators[31] also the indirect band gaps for the SiC polytypes are underestimated by the DFT-LDA procedure for the ground state by about 40–50 %.[3] At least, many-body QP effects[32] have to be taken into account to treat XC during the excitation of electrons and holes in a better way, e.g., in the *GW* approximation[33] for the self-energy, instead of by the local potential of the DFT-LDA. More strictly speaking, the validity of a perturbational approach is assumed. QP corrections $\Delta_n(\mathbf{k})$ for a certain single-particle state $|n\mathbf{k}\rangle$ (n is the band index and $\mathbf{k}$ the Bloch wave vector) are calculated as the difference between the diagonal matrix elements of the XC self-energy and the local XC potential governing the DFT-LDA. Adding the $\Delta_n(\mathbf{k})$ to the Kohn-Sham eigenvalues, one obtains the QP energies. Explicitly, we apply a generalization of the approximate procedure of the XC self-energy calculation developed by Cappellini *et al.*[34,35] for zinc-blende and diamond crystals. This procedure starts from an LDA-like treatment of the local-field contributions to the screened Coulomb potential in the *GW* approximation for the XC self-energy. The average electron density occurring in this theory is replaced by a state average of the local density. The full energy dependence of the self-energy due to the dynamical screening is described within a linear expansion around the corresponding DFT-LDA eigenvalue, which is well justified for the upper valence and lower conduction bands and not too large energy differences. The Coulomb singularity in the $\mathbf{k}$ space in the screened exchange contribution to the total self-energy is subtracted applying the concept of an auxiliary function.[36] The use of a model dielectric function,[35] which reproduces the full random-phase-approximation (RPA) function with high accuracy, allows an analytical representation of the static Coulomb-hole contribution to the self-energy. The described method represents an efficient *GW* calculation scheme for the electronic band structure of cubic semiconductors with small numbers of atoms within the unit cell. It yields accurate results with a very limited computational effort. We mention that the method of Cappellini *et al.*[34,35] is based on former simplifying approaches,[37,38] which, however, completely neglect effects of the local fields and the dynamical screening.

We have generalized the method of Cappellini *et al.*[34,35] for noncubic crystals with more than two atoms in a unit cell.[39] The diagonal (longitudinal) screening function $\epsilon^{-1}(\mathbf{q},\omega)$ is related to the inverse (transverse) dielectric tensor $\epsilon^{-1}_{\alpha\beta}(\mathbf{q},\omega)$ by $\sum_{\alpha,\beta} q_\alpha \epsilon^{-1}_{\alpha\beta}(\mathbf{q},\omega) q_\beta/|\mathbf{q}|^2$ where α and β stand for the Cartesian components. The tensor is represented in a coordinate system parallel to the principal axes. Each component is described by a model function.[35] For vanishing arguments $\epsilon^{-1}_{\alpha\beta}(0,0)$ changes over into the tensor of the inverse high-frequency dielectric constants with the independent components $\epsilon_{\perp\infty}$ and $\epsilon_{||\infty}$. The above-mentioned particular form of the inverse dielectric function guarantees its nonanalytic behavior for vanishing wave vectors. The experimental values[40] used for the parallel dielectric constants $\varepsilon_{||\infty} = 6.52$ for $3C$ and $\varepsilon_{||\infty} = 6.70$ for $6H$ are linearly interpolated with the hexagonality to the cases of $4H$ and $2H$, whereas the constant value $\varepsilon_{\perp\infty} = 6.52$ (Ref. 40) is applied to all polytypes. The auxiliary function, needed to treat the Coulomb singularity in the screened exchange contribution for the hexagonal polytypes, is chosen to be $F(\mathbf{q}) = \frac{3}{4}a^2/\{3\cos(aq_x) - 2\cos(\frac{a}{2}q_x)\cos(\frac{\sqrt{3}a}{2}q_y) + \frac{3}{2}(\frac{a}{c})^2[1-\cos(cq_z)]\}$ with the two hexagonal lattice constants a and c.[39] According to the plane-wave expansion of the single-particle states, the matrix elements of the self-energy and the local potential are represented in momentum space. Summations over the Brillouin zone are carried out using a special-point scheme.[41] Typically six (ten) mesh points are chosen in the irreducible wedge of the hexagonal (fcc) Brillouin zone to calculate the electron density. In the case of the self-energy calculation of arbitrary $\mathbf{k}$ points this number is increased to 24 in half the Brillouin zone considering only the time-reversal symmetry. The sum over reciprocal lattice vectors $\mathbf{G}$ in the shift calculation is limited by the same energy cutoff of 34 Ry as in the DFT-LDA calculations. However, much smaller values can be used to reach the same accuracy of the QP shifts. Explicitly $p\times450$ plane waves are taken into account for pH structures, whereas this number is fixed at 470 for zinc-blende SiC. The number of conduction bands plays a role. We find in the pH ($3C$) case that 128 (64) bands are required to achieve full numerical convergence of the self-energy in the considered energy range. This can be reduced to $p\times8$ (8) for pH ($3C$) in the case of the electron-density calculations.

III. RESULTS

A. Test: 3*C*-SiC

The results for the QP shifts $\Delta_n(\mathbf{k})$ for a variety of band states are summarized in Table I. Results are presented for the theoretical as well as the experimental lattice constant. They are compared with data arising from more accurate QP calculations, at the experimental lattice constant,[23,24] which take into account a full calculation of the inverse dielectric tensor within the RPA but using different methods. The overall agreement between the four different types of QP shifts is satisfying. This

TABLE I. Calculated QP shifts $\Delta_n(\mathbf{k})$ (in eV) for various band states of zinc-blende $3C$-SiC. The calculations are performed either (a) for the theoretical lattice constant or (b) for the experimental one (Ref. 40). The values are compared with results of more sophisticated calculations (Refs. 23, 24) where the experimental lattice constant is taken into account. The shifts are represented with respect to the shift of the VBM at Γ. Its absolute value is $\Delta_{15v} = -0.66$ eV (a) and $\Delta_{15v} = -0.64$ eV (b), respectively.

	QP shift			
Band state	Present (a)	Present (b)	Ref. 22	Ref. 23
Γ_{1v}	-1.63	-1.61	-1.00	-1.06
Γ_{15v}	0.00	0.00	0.00	0.00
Γ_{1c}	1.48	1.42	0.94	1.24
Γ_{15c}	1.60	1.56	1.19	1.42
X_{1v}	-1.46	-1.46	-0.93	-1.07
X_{3v}	-0.57	-0.57	-0.75	-0.68
X_{5v}	-0.22	-0.21	-0.40	-0.36
X_{1c}	1.32	1.30	1.03	1.15
X_{3c}	1.46	1.43	1.26	1.41
X_{5c}	2.38	2.33	1.73	2.12
L_{1v}	-1.50	-1.49	-0.95	-1.08
L_{1v}	-0.58	-0.57	-0.79	-0.70
L_{3v}	-0.08	-0.08	-0.15	-0.13
L_{1c}	1.45	1.40	1.07	1.30
L_{3c}	1.64	1.61	1.37	1.56
L_{1c}	2.07	2.04	1.73	1.94

holds especially for the $\mathbf{k}$ dispersion of the shifts and their dependence on the band index. With respect to the VBM the smallest shifts appear for the highest valence bands L_{3v} and X_{5v}. The strongest shifts to larger binding energies occur for the lowest valence bands L_{1v}, Γ_{1v}, and X_{1v}. They give rise to an increase of the valence band width of about 1 eV. A similar tendency is observed for the unoccupied conduction bands. There is a remarkable shift of about 1.0–1.5 eV of the lowest bands towards lower binding energies. These values increase somewhat for higher conduction bands. Compared with the band-index dependence the $\mathbf{k}$ dispersion of the shifts for a certain band is smaller. Nevertheless, it is not negligible. In the extreme cases of the higher valence bands the shift variation reaches absolute values up to 0.7 eV. Consequently, we note that the model of the "scissors" operator[42] can give a rough description of the gap opening by the QP effects but not a reasonable description of the energy bands of a rather complete QP band structure.

Comparing the absolute values of the four different types of QP calculations in Table I, one observes that in general the plane-wave description of the eigenstates (present calculation and Ref. 24) gives rise to shifts to lower (higher) binding energies for unoccupied (occupied) states which are larger than those from the wave-function expansion in terms of localized Gaussian orbitals (Ref. 23). A possible reason could be an underestimation of the interatomic contribution to the self-energy due to the stronger localization of the states. On the other hand, our model calculation gives shift values for the conduction bands and higher valence bands which are 0.1–0.2 eV larger than those of Backes *et al.*[24] We trace back this discrepancy mainly to the use of the experimental dielectric constant $\epsilon_\infty = 6.52$,[40] instead of the RPA value $\epsilon_\infty = 6.85$.[24] This gives rise to an averaged shift variation of 5%. On the other hand, the variation of the lattice constants of about 2% between the theoretical and experimental values[19] is only of minor importance for the shifts. A further reason for the discrepancies results from an overestimation of the local-field effects. The replacement of the electron density in the screening function by the state-averaged values works well for semiconductors like Si and GaAs.[34,35] However, in the case of the wide-band-gap material SiC with relatively large ionicity of the chemical bonds such a replacement leads to a slight overestimation of the shifts. The discrepancies of 0.4–0.5 eV are larger for the lowest valence band. Here the linear treatment of the energy dependence of the XC self-energy in the approximation of Cappellini *et al.*[34,35] breaks down. The dynamical screening effect has to be treated more carefully.

The band structure resulting when the QP corrections under discussion are added to the corresponding Kohn-Sham eigenvalues from the DFT-LDA is plotted in Fig. 1. Band-mapping results[12] exist for the upper valence bands along the ΓX line. We do not find complete agreement between the measured and calculated valence-band dispersions. This can be traced back to the neglect of spin-orbit coupling in our calculations, which should change the dispersion despite the smallness of the spin-orbit splitting. The QP energy eigenvalues shown in

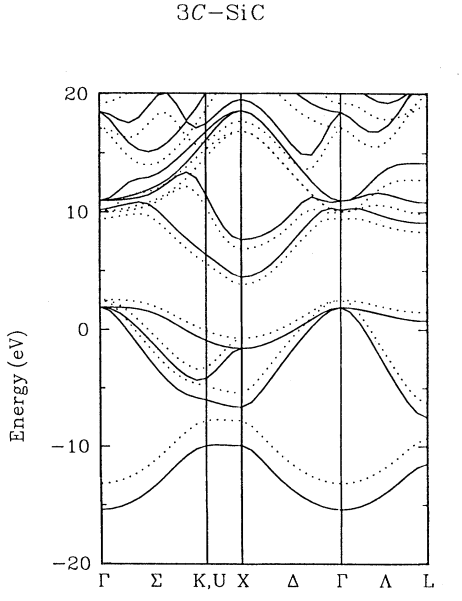

FIG. 1. The band structure of cubic $3C$-SiC within DFT-LDA (dotted lines) and after inclusion of QP corrections (solid lines). The energy zero is defined according to the asymptotic behavior of the pseudopotentials.

TABLE II. Quasiparticle energies (in eV) for 3C-SiC. For comparison with other theoretical descriptions (Refs. 23, 24) we present not only results (a) where the theoretical lattice constant is taken but also values (b) where the experimental lattice constant (Ref. 40) is used.

Band state	Present (a)	Present (b)	Ref. 23	Ref. 24	Experiment (Ref. 40)
Γ_{1v}	-17.31	-16.92	-16.44	-16.13	
Γ_{15v}	0.00	0.00	0.00	0.00	0.00
Γ_{1c}	8.29	7.67	7.35	7.81	6.00, 7.59[a]
Γ_{15c}	9.09	8.72	8.35	8.66	7.75, 8.74[a]
X_{1v}	-11.82	-11.67	-11.24	-11.19	
X_{3v}	-8.53	-8.38	-8.64	-8.38	
X_{5v}	-3.49	-3.40	-3.62	-3.42	-3.6
X_{1c}	2.59	2.59	2.34	2.37	2.390, 2.426[b]
X_{3c}	5.77	5.56	5.59	5.55	5.5, 4.7
X_{5c}	16.71	16.10	15.78	16.05	
L_{1v}	-13.39	-13.19	-12.75	-12.65	
L_{1v}	-9.39	-9.12	-9.42	-9.15	
L_{3v}	-1.13	-1.14	-1.21	-1.11	-1.16
L_{1c}	7.22	6.73	6.53	6.76	4.2
L_{3c}	8.94	8.73	8.57	8.68	8.5
L_{1c}	12.26	11.96	12.04	12.08	

[a]Values from Ref. 11.
[b]Excitonic effects are substracted.

Fig. 1 are listed in Table II for the high-symmetry points L, Γ, and X. Apart from the lowest valence band we observe a rather good agreement between the four different QP calculations. This holds especially when we also calculate the DFT-LDA eigenvalues at the experimental lattice constant. Automatically the total values decrease in agreement with the fact that the use of a smaller lattice constant corresponds to the application of hydrostatic pressure. Apart from the lowest valence band the overall agreement of the three different QP calculations is improved by changing the lattice constant in our DFT-LDA calculation to the experimental value. The only exception concerns the conduction-band minimum at X. This can be explained by the stiffness of the corresponding DFT-LDA eigenvalue against variation of the lattice constant due to the softening of the carbon pseudopotential.

Only a few band structure energies have been extracted from optical measurements. Apart from the L_{1c} state the experimental level positions at X and L can be explained by the QP eigenvalues. However, there is disagreement with older experimental data for the Γ point. The conduction-band levels, which are 6.00 or 7.75 eV above the VBM and have been identified with s-like (Γ_{1c}) or p-like (Γ_{15c}) states, lie already higher in energy than the corresponding DFT-LDA eigenvalues. A critical discussion of this fact is given in the paper of Rohlfing *et al.*[23] On the other hand, the same level positions recalculated by Lambrecht *et al.*[11] from recent reflectivity measurements agree excellently with our predictions at the experimental lattice constant.

B. Influence of hexagonality

The variety of QP shifts calculated for the hexagonal polytypes at the high-symmetry points Γ, K, H, A, M, and L in the hexagonal Brillouin zone are represented in Fig. 2 together with those for 3C-SiC versus the corresponding DFT-LDA energies. One observes no clear behavior within the different groups of bands. On the average, the positive (negative) QP shifts increase with

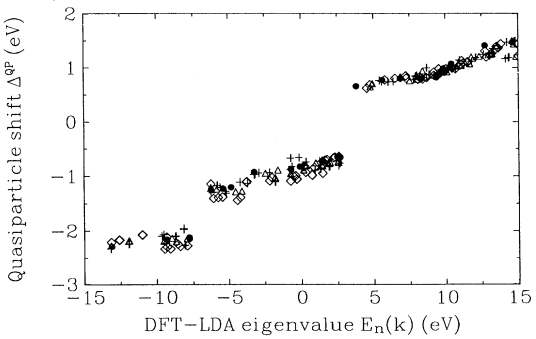

FIG. 2. Quasiparticle shifts versus DFT-LDA energies for the polytypes under consideration. The asymptotics of the pseudopotentials is used as a unique energy zero for all polytypes. The following high-symmetry points are selected: Γ, $K(U)$, X, and L for 3C; A, L, $\frac{2}{3}LM$, M, Γ, H, and K for 2H; M and Γ for 4H as well as 6H. 3C: dots, 2H: crosses, 4H: triangles, 6H: diamonds.

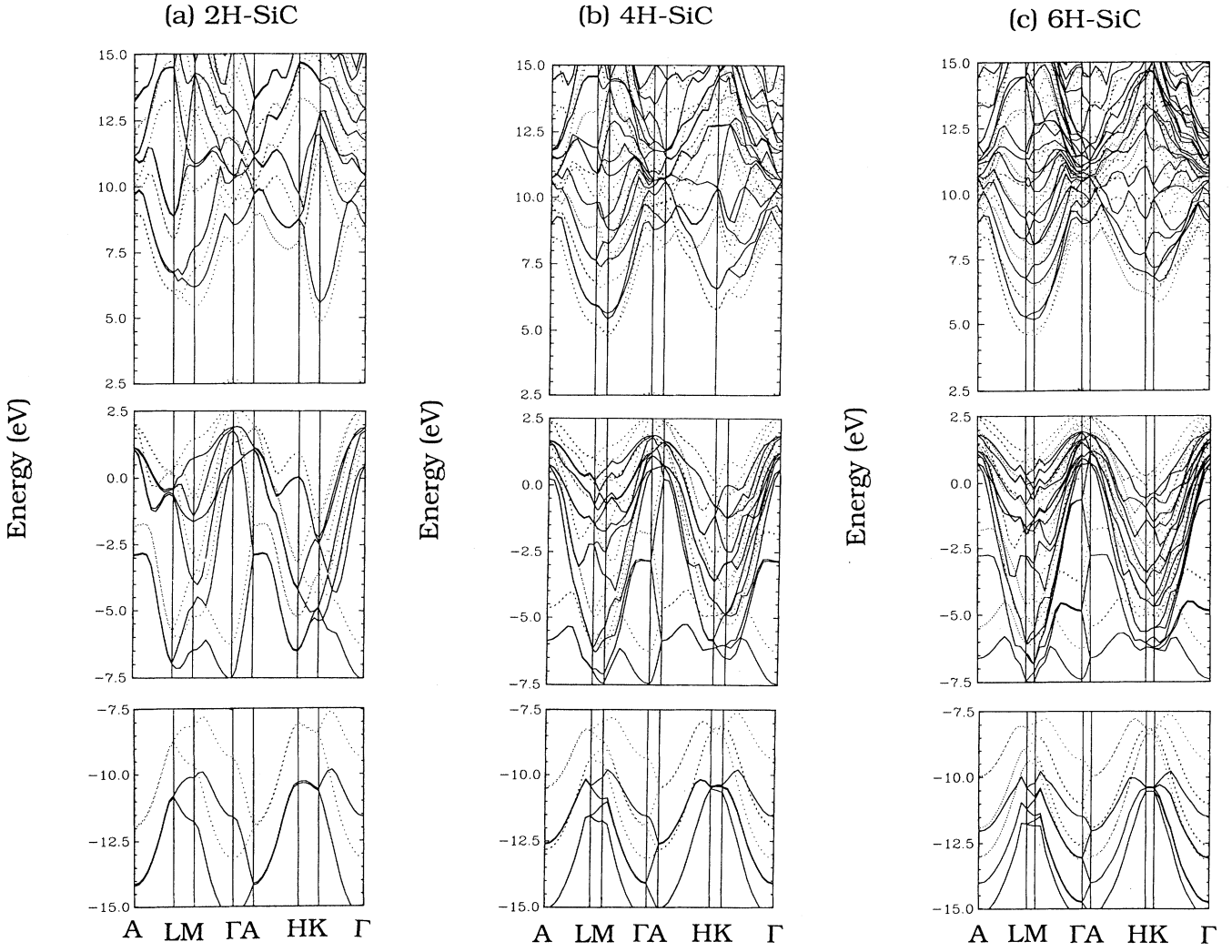

FIG. 3. Quasiparticle (solid lines) and DFT-LDA (dashed lines) band structures for the hexagonal SiC polytypes $2H$ (a), $4H$ (b), and $6H$ (c). Because of the variety of bands, different energy regions of the band structures are plotted in different panels. The zero of the pseudopotentials is used as the energy zero for all polytypes.

the distance of the conduction- (valence-) band state from the fundamental energy gap. The shifts exhibit a steplike behavior in the regions of the ionic energy gap in the valence bands as well as of the fundamental gap. Consequently, the application of one energy-independent scissor operator is impossible to bring the DFT-LDA band structure into agreement with experimental findings. In particular, Fig. 2 makes evident the discontinuity of the shifts in the region of the fundamental indirect gap as well as the ionic gap. We find openings of the indirect gaps due to the QP effects by 1.30 eV ($3C$), 1.26 eV ($6H$), 1.35 eV ($4H$), and 1.52 eV ($2H$). Their variation with the hexagonality of the polytype is small. The main reason for the discrepancy between the value for $2H$ and the other ones arises from the different location of the conduction-band minima in $\mathbf{k}$ space.

The QP band structures resulting for $2H$, $4H$, and $6H$ are represented in Fig. 3 along high-symmetry lines in the hexagonal Brillouin zone together with the underlying DFT-LDA ones. The corresponding band-structure energies are listed in Table III, at least for the high-symmetry points and the bands around the fundamental gap. In agreement with the representation of the $3C$-SiC band structure in a $3H$ Brillouin zone, where the conduction-band minimum appears at the M point,[3] the conduction-band minima for the polytypes $6H$ and $4H$ with low percentage hexagonality appear at the M point. There are experimental reasons[25] to believe that in the $4H$ case the minimum is located at an F position instead of at M or the LM line in the hexagonal Brillouin zone. However, we cannot find an indication for the minimum location at a $\mathbf{k}$ point in the plane surrounded by the points Γ, A, L, and M, neither in the DFT-LDA band structure nor after inclusion of QP effects. In both band structures we find the minimum at the M point in agreement with further DFT-LDA calculations.[3,18,20,21] On the other hand, for

TABLE III. Band structure energies (in eV) at high-symmetry points Γ, K, H, A, M, and L in the hexagonal Brillouin zone within the DFT-LDA and including the QP shift. Only the uppermost valence band and the lowest conduction band are given. In addition, the lowest valence level Γ_{1v} is indicated to characterize the valence-band width. For comparison the zinc-blende band structure is also represented within the hexagonal Brillouin zone ($3H$). The symmetry notation of Rashba (Ref. 43) is used.

Band state	$6H$		$4H$		$3H$		$2H$	
	LDA	QP	LDA	QP	LDA	QP	LDA	QP
Γ_{1v}	-15.71	-17.28	-15.74	-17.30	-15.68	-17.20	-15.83	-17.39
Γ_{6v}	0.00	0.00	0.00	0.00	0.00	0.00	0.00	0.00
Γ_{1c}	5.53	6.95	5.43	6.92	6.01	7.62	5.11	6.66
K_{2v}	-2.09	-2.31	-1.67	-1.85	-2.22	-2.36	-3.95	-4.12
K_{2c}	3.45	4.88	3.93	5.45	3.81	5.41	2.14	3.68
H_{3v}	-2.30	-2.49	-2.49	-2.68	-3.23	-3.34	-1.71	-1.83
H_{3c}	3.63	5.06	3.19	4.68	5.12	6.78	5.26	6.86
$A_{5,6v}$	-0.09	-0.09	-0.19	-0.20	-0.34	-0.31	-0.69	-0.75
$A_{1,3c}$	5.59	7.02	5.64	7.14	5.77	7.35	6.18	7.81
M_{4v}	-1.10	-1.40	-1.12	-1.23	-1.80	-1.82	-1.19	-1.13
M_{1c}	1.99	3.25	2.21	3.56	1.26	2.69	2.76	4.28
$L_{1,2,3,4v}$	-1.31	-1.63	-1.55	-1.68	-1.05	-1.03	-2.33	-2.30
$L_{1,3c}$	2.05	3.36	2.63	4.06	2.68	4.22	3.34	4.85

$4H$ we observe a rather pronounced flatness of the lowest conduction band in the **k** space direction towards the next-neighbor M' point in the Brillouin zone. However, this indication for an additional minimum is widely lifted after inclusion of QP effects. In the $6H$ case the situation is less clear. Several recent DFT-LDA calculations[3,20,21] but not all[18] find the minimum to occur at the LM line. Such a theoretical **k** space position seems to be in agreement with experimental conclusions from phonon energies involved in luminescence replicas[44] as well as considerations of the Kohn-Luttinger interference effect.[45] We find a dependence of this lowest conduction band and its minimum position on the numerical details, the convergency of the energy-minimization procedure to determine the bands or the inclusion of QP effects. This sensitivity of its **k** space location to the details of the electronic-structure calculations is studied in more detail in Fig. 4 for the flat lowest conduction band along LM in $6H$. With increasing number of time steps taken into the Car-Parrinello-like energy-minimization procedure we find a displacement of the considered minimum towards M. Simultaneously, the nonparabolicity of the considered conduction band diminishes. The convergency of the result is checked by comparison with a direct diagonalization. We find agreement after 240 time steps in the Car-Parrinello procedure. The sensitivity itself can be understood in terms of the flatness of the band along LM. The **k** dispersion of a band of about 0.01 eV approaches or even undercuts the accuracy of the underlying DFT-LDA calculation and much more that of 0.1 eV of our QP calculation. After inclusion of QP effects we find an even stronger tendency to stabilize the conduction-band minimum at M and an upward shift of about 0.6 eV. It is accompanied by a slight change of the band curvature.

Together with the generally accepted position at K for the conduction-band minimum in the wurtzite $2H$ structure a clear picture of the dependence of the indirect energy gap on the percentage hexagonality of the poly-

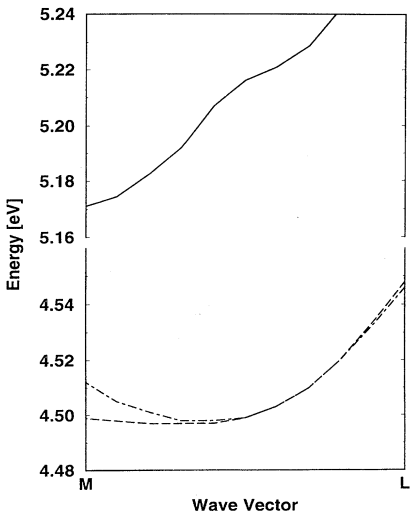

FIG. 4. Lowest conduction band of $6H$-SiC along the LM line resulting from a QP calculation and different DFT-LDA calculations which take into account different numbers N_T of time steps in the indirect diagonalization procedure. QP: solid line ($N_T = 240$), DFT-LDA: dashed line ($N_T = 240$), dot-dashed line ($N_T = 60$).

type follows from the calculations. For 0% hexagonality (3C-SiC) the lowest conduction-band minimum starts at X (fcc Brillouin zone) or M (3H Brillouin zone) roughly 2.59 eV above the VBM. The minimum in 6H (33%) appears at an energetic distance of about 3.25 eV at M. This value increases somewhat in the 4H case (50% hexagonality). This behavior of the lowest conduction-band state in the **k** and energy space explains the experimental findings, the so-called Choyke-Hamilton-Patrick relation.[1] Certainly, our theoretical values slightly overestimate the transition energies compared with the experimental values[40] 2.390 eV (3C), 3.023 eV (6H), 3.265 eV (4H), and 3.330 eV (2H). However, the agreement can be improved when the exciton binding energies of the order of 0.03–0.05 eV (Ref. 40 and interpolated) are added to the experimental values and the DFT-LDA eigenvalues are calculated at the experimental atomic positions and not at equilibrium positions which minimize the total electronic energy. The remaining discrepancy of about 0.1 eV can be traced back to the inaccuracies in our shift calculations which can be lifted by a more proper treatment of the local-field contributions to the XC self-energy.

C. QP influence on band discontinuities and electron effective masses

There is an ongoing debate concerning the existence of novel electronic properties of heterostructures (more strictly speaking heterocrystalline structures) on a base of different SiC polytypes. Two extreme points of view occur. On the one hand, the viewed structures should have properties like heterostructures on a base of different materials. On the other hand, these structures give rise to new polytypes with averaged properties. The most interesting heterocrystalline structures are those between 3C with a small energy gap and a pH structure with a much larger gap. The most characteristic parameters of such heterostructures are the band discontinuities ΔE_v between the valence-band maxima (VBM) at Γ and ΔE_c between the minima at X (3C) and M (4H, 6H) or K (2H). Under the assumption that interface dipoles are negligible, they can easily be determined since the asymptotics of the pseudopotentials define a unique reference level for all combinations as indicated in the band structures of Figs. 1 and 3. The dipoles are indeed expected to be small in view of the similarity in charge density and bonding in the polytypes. This seems to be also confirmed by the 3C/2H calculation of Ref. 46. For the combinations 3C/pH we find $\Delta E_c = 0.74$ eV ($p = 6$) and 0.99 eV ($p = 4$ and 2) as well as $\Delta E_v = -0.02$ eV ($p = 6$), –0.05 eV ($p = 4$), and –0.13 eV ($p = 2$) indicating type-II heterostructures with pronounced electron wells in the 3C layers and flat hole wells in the pH polytype. These values are modified after inclusion of the QP effects, to $\Delta E_c = 0.70$ eV ($p = 6$), 0.97 eV ($p = 4$), and 1.10 eV ($p = 2$), and $\Delta E_v = 0.00$ eV ($p = 6$), – 0.10 eV ($p = 4$), and –0.24 ($p = 2$), respectively. In general, the QP corrections increase the type-II character of the considered heterostructural combinations. The hole wells are more pronounced and the effective gap of the total system is decreased.

TABLE IV. Effective masses of electrons in the conduction-band minima in units of the free-electron mass m_0. For comparison the values neglecting the quasiparticle effect are given in parentheses. Full converged DFT-LDA bands are taken into account. Only the independent components of the tensors are presented. The principal axes ($||$ and $\perp$) are $X\Gamma$ [001] and XU [1$\bar{1}$0] (3C), KH [0001] and $K\Gamma$ [11$\bar{2}$0] (2H), and ML [0001] and $M\Gamma$ [1$\bar{1}$00] (4H, 6H). Since the little group of the M point (C_{2v}) is smaller than that for the K point (C_{3v}), a second perpendicular mass along MK [11$\bar{2}$0] is given for 4H as well as 6H.

Mass	3C (X)	6H (M)	4H (M)	2H (K)
$m_{\|\|}$	0.67	0.51	0.19	0.25
	(0.67)	(1.95)	(0.32)	(0.26)
$m_\perp$	0.24	0.71	0.60	0.43
	(0.25)	(0.75)	(0.57)	(0.45)
		0.30	0.28	
		(0.27)	(0.32)	

The influence of the QP effect on the effective masses and, hence, the **k** dispersion vary with the polytype and the extremum under consideration. We discuss this effect for the conduction-band minima. The corresponding results are listed in Table IV. This table presents the independent components of the effective-mass tensor with principal axis parallel to the c axis (hexagonal polytypes) or to the $X\Gamma$ connection line (zinc blende) and, respectively, perpendicular to these directions. In general, the QP influence is weak and give rise mostly to a rather small decrease in comparison to the DFT-LDA values. In the case of the well established minima at X or K in 3C-SiC and 2H-SiC, respectively, the QP influence on the effective masses of the electrons is really negligible. The strongest changes happen for $m_{||}$ of 4H and, in particular, 6H. The underlying reason, the sensitivity of the bands parallel to the ML line to the details of the numerical calculation, has been already discussed above. Small **k**-dependent shifts of the energies of the flat band along ML give rise to drastic changes of its curvature.

The agreement with the available data from cyclotron-resonance measurements for 3C-, 6H-, and 4H-SiC (Refs. 13–15) is satisfying. We find for the $X\Gamma$ and XU directions in 3C the values $m_{||} = 0.67m_0$ and $m_\perp = 0.24m_0$. There is practically no variation of these values with the QP effect or with the numerical details of the calculation, especially the number of time steps taken into account. The two values are in excellent agreement with the observations in Ref. 13. The longitudinal mass $m_{||} = 0.67m_0$ is exactly reproduced, whereas in the perpendicular case the experimental value $m_\perp = 0.25m_0$ is slightly underestimated after the inclusion of QP effects. In the 6H case the measured values are $m_{||} = 2.0m_0$ and $m_\perp = 0.42m_0$.[14] These values are in very good agreement with the DFT-LDA findings in Table IV. However, for the parallel mass the small wave-vector dispersion of the QP correction perturbs the agreement. On the other

hand, the experimental value for $m_\perp$ lies in between the two theoretical ones in the DFT-LDA as well as the QP case. For $4H$ the measured values are $m_{||} = 0.29m_0$ and $m_\perp = 0.42m_0$.[15] The first value lies in between our DFT-LDA and QP results. The second one seems to approach the average value of the two transverse masses given in Table IV. In any case the theory confirms that, in contrast to $6H$, the mass parallel to the c axis is the smallest one in a $4H$ polytype. Assuming an electron movement in the basal plane in the $[11\bar{2}0]$ direction and a relation $\mu_\perp/\mu_{||} = m_{||}/m_\perp$, i.e., neglecting the anisotropy in the electron scattering, the anisotropy of the electron mobility is reproduced in the case of Ref. 14 ($\mu_\perp/\mu_{||} = 0.69$) whereas another $4H$ value $\mu_\perp/\mu_{||} = 0.83$ (Ref. 47) is underestimated. Very recently we received unpublished $4H$ data, $m_{||} = 0.33m_0$, $m_{\perp 1} = 0.58m_0$, and $m_{\perp 2} = 0.31m_0$,[48] where the directions are specified. These masses are in excellent agreement with our DFT-LDA values in Table IV. The same holds for the QP-corrected bands. Only in the ML direction is the discepancy larger for reasons discussed above. The masses $m_{||} = 0.22m_0$ ($0.34m_0$) and $m_\perp = 0.18m_0$ ($0.24m_0$), deduced recently from an effective-mass approximation fitted to the spectra of the excited states of nitrogen donors for $4H$ ($6H$) in Refs. 49 (50), fail the comparison. On the other hand, the anisotropy of the electron masses for $6H$ still remains a problem. The remarkable anisotropy of $m_{||}/m_\perp \approx 4$ found in cyclotron-resonance studies[48] can be reproduced within our DFT-LDA treatment, at least for an average of the perpendicular masses. However, it cannot be confirmed after inclusion of the QP effects. Unfortunately, the accuracy of the QP effects for the flat conduction band along LM is not high enough to give an ultimate conclusion. Minor changes of the QP shifts for different **k** points give rise to remarkable changes of the band dispersion in the flat-band case.

IV. SUMMARY

In conclusion, we have studied the electronic excitation properties of various SiC polytypes combining the first-principles pseudopotential method in the framework of DFT-LDA with a proper calculation of the quasiparticle effects. We have shown that the simplifying treatment of Cappellini *et al.* of the XC self-energy within the GW approximation is sufficient for near-band-gap excitations. At the experimental lattice parameters we found an accuracy of about 0.1 eV. It can be improved by a more careful treatment of the local-field contributions to the screened potential in these wide-band-gap semiconductors.

The resulting QP shifts of the DFT-LDA bands vary with the polytype, the band index, and the position of the Bloch state within the Brillouin zone. A scissor operator can indicate the tendency of the opening of the band gaps. However, by no means is it able to explain the details of the quasiparticle band structures. They concern the **k** space location of the band extrema, the exact magnitude of the band discontinuities of structures based on different SiC polytypes, as well as the curvature of bands, or more strictly speaking the corresponding effective masses. The results presented allow an explanation of the trend of the energy gaps with the hexagonality as well as the absolute magnitude of these energies.

ACKNOWLEDGMENTS

We thank R. Del Sole, R. P. Devaty, and B. K. Meyer for helpful discussions. The work was supported by the Sonderforschungsbereich 196 (Project A08) of the Deutsche Forschungsgemeinschaft and the EC Programme Human Capital and Mobility under Contract No. ERBCHRXCT 930337.

[1] W.J. Choyke, D.R. Hamilton, and L. Patrick, Phys. Rev. **133**, 1163 (1964).
[2] L. Patrick, D.R. Hamilton, and W.J. Choyke, Phys. Rev. **143**, 526 (1966).
[3] P. Käckell, B. Wenzien, and F. Bechstedt, Phys. Rev. B **50**, 10 761 (1994).
[4] W.H. Backes, P.A. Robbert, and W. van Haeringen, Phys. Rev. B **49**, 7564 (1994).
[5] B.E. Wheeler, Solid State Commun. **4**, 173 (1966).
[6] S. Logothetidis, H.M. Polatoglou, J. Petalas, D. Fuchs, and D.R. Johnson, Physica B **185**, 389 (1993).
[7] V.I. Gavrilenko, S.I. Frolov, and N.I. Klyui, Physica B **185**, 394 (1993).
[8] W.J. Choyke and L. Patrick, Phys. Rev. **172**, 769 (1968).
[9] V.V. Makarov, Fiz. Tekh. Poluprovodn. **6**, 1805 (1972) [Sov. Phys.- Semicond. **6**, 1556 (1973)].
[10] V. Rehn, J.L. Stanford, V.O. Jones, and W.J. Choyke, in *Proceedings of the 13th International Conference on the Physics of Semiconductors, Rome, 1976*, edited by F.G. Fūmi (Marves, Rome, 1976), p. 985.
[11] W.R.L. Lambrecht, B. Segall, M. Suttrop, M. Yoganathan, R.P. Devaty, W.J. Choyke, J.A. Edmond, J. A Powell, and M. Alouani, Appl. Phys. Lett. **63**, 2747 (1993); Phys. Rev. B **50**, 10 722 (1994).
[12] H. Höchst and M. Tang, J. Vac. Sci. Technol. A **5**, 1640 (1987).
[13] R. Kaplan, R.J. Wagner, H.J. Kim, and R.F. Davis, Solid State Commun. **55**, 67 (1985).
[14] N.T. Son, O. Kordina, A.O. Konstantinov, W.M. Chen, E. Sörman, B. Monemar, and E. Janzen, Appl. Phys. Lett. **65**, 3209 (1994).
[15] N.T. Son, W.M. Chen, O. Kordina, A.O. Konstantinov, B. Monemar, E. Janzen, D.M. Hofmann, D. Volm, M. Drechsler, and B.K. Meyer, Appl. Phys. Lett. **66**, 1074 (1995).
[16] C. Cheng, R.J. Needs, V. Heine, and N. Churcher, Europhys. Lett. **3**, 475 (1987); J. Phys. C **21**, 1049 (1988); C. Cheng, V. Heine, and R.J. Needs, J. Phys. Condens. Matter **2**, 5115 (1990).
[17] W.R.L. Lambrecht, B. Segall, M. Methfessel, and M. van Schilfgaarde, Phys. Rev. B **44**, 3685 (1991).

[18] C.H. Park, B.-H. Cheong, K.-H. Lee, and K.J. Chang, Phys. Rev. B **49**, 4485 (1994); Solid State Commun. **92**, 869 (1994).
[19] P. Käckell, B. Wenzien, and F. Bechstedt, Phys. Rev. B **50**, 17 039 (1994).
[20] K. Karch, G. Wellenhofer, P. Pavone, U. Rössler, and D. Strauch, in *Proceedings of the 22nd International Conference on the Physics of Semiconductors, Vancouver, 1994*, edited by D.J. Lockwood (World Scientific, Singapore, 1995), p. 401.
[21] W.R.L. Lambrecht, in *Diamond, SiC and Nitride Wide Bandgap Semiconductors*, edited by C.H. Carter, Jr., G. Gildenblat, S. Nakamura, and R.J. Nemanich, MRS Symposia Proceedings No. 339 (Materials Research Society, Pittsburgh, 1994), p. 565.
[22] L. Wenchang, Z. Kaining, and X. Xide, J. Phys. Condens. Matter **5**, 883 (1993).
[23] M. Rohlfing, P. Krüger, and J. Pollmann, Phys. Rev. B **48**, 17 791 (1993).
[24] W.H. Backes, P.A. Bobbert, and W. van Haeringen, Phys. Rev. B **51**, 4960 (1995).
[25] L. Patrick, W.J. Choyke, and D.R. Hamilton, Phys. Rev. **137**, A1515 (1965).
[26] G.B. Bachelet, D.R. Hamann, and M. Schlüter, Phys. Rev. B **26**, 4199 (1982).
[27] L. Kleinman and D.M. Bylander, Phys. Rev. Lett. **48**, 1425 (1982).
[28] B. Wenzien, P. Käckell, and F. Bechstedt, Surface Sci. **307–309**, 989 (1994).
[29] R. Stumpf and M. Scheffler, Comput. Phys. Commun. **79**, 447 (1994).
[30] R. Car and M. Parrinello, Phys. Rev. Lett. **55**, 2471 (1985).
[31] F. Bechstedt, Adv. Solid State Phys. **32**, 161 (1992).
[32] M.S. Hybertsen and S.G. Louie, Phys. Rev. B **34**, 5390 (1986).
[33] L. Hedin and S. Lundqvist, Solid State Phys. **23**, 1 (1969).
[34] F. Bechstedt, R. Del Sole, G. Cappellini, and L. Reining, Solid State Commun. **84**, 765 (1992).
[35] G. Cappellini, R. Del Sole, L. Reining, and F. Bechstedt, Phys. Rev. B **47**, 9892 (1993).
[36] F. Gygi and A. Baldereschi, Phys. Rev. B **34**, 4405 (1986).
[37] F. Bechstedt and R. Del Sole, Phys. Rev. B **38**, 7710 (1988).
[38] F. Gygi and A. Baldereschi, Phys. Rev. Lett. **62**, 2160 (1989).
[39] B. Wenzien, G. Cappellini, and F. Bechstedt, Phys. Rev. B **51**, 14 701 (1995).
[40] *Semiconductors Physics of Group IV Elements and III-V Compounds*, edited by K.-Hellwege and O. Madelung, Landolt-Börnstein, New Series, Group III, Vol. 17, Pt. a (Springer, Berlin, 1982); Vol. 22, Pt. a (Springer, Berlin, 1987).
[41] D.J. Chadi and M.L. Cohen, Phys. Rev. B **8**, 5747 (1973).
[42] G. Baraff and M. Schlüter, Phys. Rev. B **30**, 3460 (1984).
[43] E.I. Rashba, Fiz. Tverd. Tela (Leningrad) **1**, 407 (1959) [Sov. Phys. Solid State **1**, 2569 (1960)].
[44] W.J. Choyke and L. Patrick, Phys. Rev. **127**, 1868 (1962).
[45] L. Patrick, Phys. Rev. B **5**, 2198 (1972).
[46] A. Qteish, V. Heine, and R.J. Needs, Phys. Rev. B **45**, 6534 (1992).
[47] W.J. Schaffer, G.H. Negley, K.G. Irvin, and J.W. Palmour, in *Diamond, SiC and Nitride Wide Bandgap Semiconductors* (Ref. 21), p. 595.
[48] D.M. Hofmann and B.K. Meyer (private communication).
[49] W. Suttrop, G. Pensl, W.J. Choyke, R. Stein, and S. Leibenzeder, J. Appl. Phys. **72**, 3708 (1992).
[50] W. Götz, A. Schöner, G. Pensl, W. Suttrop, W.J. Choyke, R. Stein, and S. Leibenzeder, J. Appl. Phys. **73**, 3332 (1993).